Journal of Nuclear Materials 384 (2009) 322–326

Contents lists available at ScienceDirect

Journal of Nuclear Materials

journal homepage: www.elsevier.com/locate/jnucmat

Titanate ceramics for immobilisation of uranium-rich radioactive wastes arising from ^{99}Mo production

M.L. Carter, H. Li, Y. Zhang *, E.R. Vance, D.R.G. Mitchell

Institute of Materials Engineering, Australian Nuclear Science and Technology Organisation, PMB 1, Menai, Sydney, NSW 2232, Australia

ARTICLE INFO

Article history:
Received 8 August 2008
Accepted 5 December 2008

ABSTRACT

Uranium-rich liquid wastes arising from UO_2 targets which have been neutron-irradiated to generate medical radioisotopes such as ^{99m}Tc require immobilisation. A pyrochlore-rich hot isostatically pressed titanate ceramic can accommodate at least 40 wt% of such waste expressed on an oxide basis. In this paper, the baseline waste form composition (containing 40 wt% UO_2) was adjusted in two ways: (a) varying the UO_2 loading with constant precursor oxide materials, (b) varying the precursor composition with constant waste loading of UO_2. This resulted in the samples having a similar phase assemblage but the amounts of each phase varied. The oxidation states of U in selected samples were determined using diffuse reflection spectroscopy (DRS) and electron energy loss spectroscopy (EELS). Leaching studies showed that there was no significant difference in the normalised elemental release rates and the normalised release rates are comparable with those from synroc-C. This demonstrates that waste forms based on titanate ceramics are robust and flexible for the immobilisation of U-rich waste streams from radioisotope processing.

1. Introduction

Molybdenum-99 (^{99}Mo) and its daughter product ^{99m}Tc are among the most important radionuclides used in nuclear medicine [1] insofar as ^{99m}Tc is used in about 80% of all radiodiagnostic medicine. Radioactive wastes arising from the production of ^{99}Mo must be appropriately managed. ^{99}Mo for medical purposes is produced mainly by the nuclear fission of ^{235}U and there are a number of techniques to separate out ^{99}Mo [2–9]. In this present work, the focus is the intermediate-level uranium-rich radioactive waste arising from the reactor irradiation of ~2% enriched UO_2 targets, with the targets being dissolved in concentrated nitric acid. The resulting solution is passed through an Al_2O_3 column where the ^{99}Mo is absorbed and the remaining solution containing U and the rest of the fission products constitutes the U-rich waste stream. The waste under consideration here would have a specific activity of order 1 Ci/L (after storage for ~10 years) and be designated as intermediate-level waste in Europe, but the specific activity is comparable to that of US Tank wastes arising from weapons production in the United States and designated as high-level waste (HLW) in that country. Hence regulatory tests appropriate to HLW should be appropriate, if perhaps somewhat conservative, to form part of the validation of candidate waste forms. Options for immobilisation of this waste could include cementation after years of cooling. However, in the present work we focus on titanate ceramics of the synroc type [10]. On an oxide basis (neglecting water, nitric acid and other entities that can be removed by calcination) the waste would typically contain >95 wt% of UO_x, plus process chemicals, and ~0.2 wt% fission products. The nearest type of waste for which the synroc family of titanate ceramics has been previously targeted is dissolved spent fuel, and the corresponding synroc variant is synroc-F [11]. Synroc-F consists of 85 wt% of pyrochlore-structured $CaUTi_2O_7$, plus 5 wt% each of perovskite, hollandite and rutile. Vance et al. [12] designed pyrochlore-rich waste forms containing between 25 and 44 wt% UO_2 to immobilise the U-rich waste from ^{99}Mo production. The pyrochlore-rich waste form contained 80 wt% pyrochlore and 10 wt% each of rutile and hollandite.

The difference between the two applications is that spent fuel contains roughly 3 wt% of fission products, necessitating the presence of perovskite to incorporate Sr, whereas the waste form from radioisotope production contains much less (~0.2 wt%) fission product. Hence Sr can be incorporated in the hollandite or, if not, can react with the excess rutile to form a very small amount of perovskite. Vance et al. [12] concluded that the pyrochlore-rich waste forms containing between 25 and 44 wt% UO_2 have excellent aqueous durability, comparable to that of synroc-C [13]. The 'baseline' waste form composition contained 40 wt% UO_2 in a matrix consisting of around 80 wt% pyrochlore, 10 wt% rutile and 10 wt% hollandite. The nominal composition for the pyrochlore was $CaU_{0.86}Zr_{0.14}Ti_2O_7$, with U in the 4+ state and that of the hollandite was $Ba_{1.2}Al_{2.4}Ti_{5.6}O_{16}$.

* Corresponding author. Tel.: +61 2 9717 9156; fax: +61 2 9543 7179.
E-mail address: yzx@ansto.gov.au (Y. Zhang).

0022-3115/$ - see front matter © 2009 Elsevier B.V. All rights reserved.
doi:10.1016/j.jnucmat.2008.12.042

In the current work, we investigate the compositional flexibility of pyrochlore-rich waste forms to incorporate the U-rich waste from ^{99}Mo production, in terms of phase development and aqueous durability by adjusting the waste form composition in two ways: (a) varying the UO_2 loading while keeping the precursor oxide material constant, and (b) varying the precursor composition while keeping the waste loading of UO_2 constant.

2. Experimental

Table 1 lists the compositions of the samples used in this work. The samples were prepared by a modified alkoxide-route. This involves the following steps. The correct molar quantities of titanium (IV) isopropoxide, aluminum sec-butoxide and zirconium tertbutoxide in ethanol (~100 ml ethanol per 100 g of alkoxides) were mixed with the other nitrates (Ca^{2+}, Ba^{2+} and UO_2^{2+}) dissolved in water (~200 ml water per 100 g of nitrates). The two solutions were then intimately combined in a stainless steel beaker using a shear mixer. The mixture was then heated to dryness in the stainless steel beaker on a hot plate at ~90 °C. The dry product was transferred to an alumina crucible and calcined in 3.5% H_2/N_2 for 1 h at 750 °C. The calcined powder was wet ball milled in Teflon containers using yttria stabilised zirconia balls in water with rotation at ~75 rpm for 16 h. The milled powder and liquid were separated from the balls by pouring through a plastic colander. The powder and liquid were recombined and dried at ~110 °C in a stainless steel vessel. About 2 wt% Ti metal powder (<325 μm) was added and mixed with all powders, then the powders were sealed in stainless steel cans evacuated at 400 °C. The samples were then hot isostatically pressed (HIPed) at 1200 °C under an argon atmosphere (100 MPa) for 1 h.

The chemical durability of the samples was estimated using the product consistency test (PCT), test method B [14]. In this test method, the sample is crushed and sieved to U.S. Standard ASTM −100 to −200 mesh (0.149–0.074 mm). The particles were cleaned of adhering fines by washing in cyclohexane, and ~1 g of sized and cleaned material was placed in a polytetrafluoroethylene-lined vessel. An amount of deionised water equal to 10 ± 0.5 cm^3/g of sample mass was added and the vessel sealed. The vessel was placed in an oven at 90 ± 2 °C. After 7 days, the vessel was removed from the oven and cooled to ambient temperature. Leachate solutions were removed from the powder and run through a 45 μm filter, and then analysed for the elements of interest using a Perkin–Elmer PE-SCIEX Elan 6000 inductively coupled plasma-mass spectrometer (ICP-MS).

A JEOL JSM6400 scanning electron microscope (SEM) operating at 15 kV, and equipped with a Noran Voyager energy-dispersive spectroscopy system (EDS) was used for microstructural analysis and characterisation. X-ray diffraction (XRD) was carried out using a Philips PW1050 with Cu Kα radiation; data were collected over the angular range $5° \leqslant 2\Theta \leqslant 85°$ with a step size of 0.05° and an acquisition time of 5 s per step. Samples were crushed (~30 μm) for the XRD work. The XRD patterns were analysed using PANalytical X'Pert HighScore software using the semi-quantitative analysis feature. The semi-quantitative analysis feature calculates the estimated mass fraction of each phase.

Diffuse reflectance (DR) spectra were collected at ambient temperature using a Cary 500 spectrophotometer equipped with a Labsphere Biconical Accessory. Spectra are referenced to that of a Labsphere certified standard (Spectralon), and transformed into Kubelka–Munk units, $F(R) = (1 - R)^2/2R$ [15]. Electron energy loss spectroscopy (EELS) was carried out on a JEOL 2010F TEM operated at 200 kV, and fitted with Gatan imaging filter. Uranium valence was determined by capturing EELS spectra of the Uranium M5 and M4 edges at an energy loss of 3552 and 3728 eV, respectively. Spectra were captured using the conditions employed by Colella et al. [16], who determined the relationship between the branching ratio ([M5 intensity]/[M5 intensity + M4 intensity]) and the valence state of a series of U-containing reference materials. Use was made of this relationship in determining the valence state of the U-containing phases investigated here from their measured branching ratio.

3. Results and discussion

3.1. Varying the waste loading

The waste loading was varied from 30 to 45 wt%, in samples where the precursor oxide material was kept constant (see Table 1), with the baseline composition being 40 wt% UO_2.

The samples containing 30, 35, 40 and 45 wt% UO_2 were examined by XRD after HIPing. The baseline composition (40 wt% UO_2, sample 2 in Table 1) showed the sample to contain pyrochlore (71%), rutile (15%), hollandite (10%) and brannerite (UTi_2O_6, 4%). The baseline sample was not designed to contain brannerite, however, brannerite is commonly found in pyrochlore-rich ceramics [12,17–19], and the effect of brannerite on the aqueous durability of the waste form will be discussed later. Fig. 1 shows the backscattered electron image of the baseline sample. Phases identified by SEM were pyrochlore, rutile, hollandite and a small amount of brannerite as predicted by the XRD analysis. The sample was fully dense and grain size was <1 μm, consistent with hot pressed synroc-C [10].

The XRD data showed the samples containing 30 and 35 wt% UO_2 (samples 3 and 1, respectively, in Table 1) consisted of pyrochlore, rutile, hollandite and perovskite ($CaTiO_3$), with the 30 wt% UO_2 sample containing more perovskite (14%) as against 4% in the 35% UO_2-containing sample (see Table 2) The presence of

Table 1
Compositions of the samples.

Oxide	Same precursor with different UO_2 content				Same UO_2 content with different precursor			
	Sample number 1 (wt%)	Sample number 2 (wt%)	Sample number 3 (wt%)	Sample number 4 (wt%)	Sample number 5 (wt%)	Sample number 6 (wt%)	Sample number 7 (wt%)	Sample number 8 (wt%)
CaO	10.47	9.66	11.27	8.86	7.73	6.76	13.73	15.76
Al_2O_3	1.69	1.56	1.82	1.43	1.25	1.09	1.25	1.09
BaO	2.54	2.34	2.73	2.15	1.87	1.64	1.87	1.64
ZrO_2	3.19	2.94	3.43	2.70	2.35	2.06	2.35	2.06
TiO_2	47.19	43.56	50.82	39.93	46.84	48.49	40.84	39.49
UO_2	35.00	40.00	30.00	45.00	40.00	40.00	40.00	40.00
Notes all in weight %	65 precursor 35 UO_2	'Baseline': 60 precursor 40 UO_2	70 precursor 30 UO_2	55 precursor 45 UO_2	48 precursor 40 UO_2 12 TiO_2	42 precursor 40 UO_2 18 TiO_2	48 precursor 40 UO_2 6 TiO_2 6 CaO	42 precursor 40 UO_2 9 TiO_2 9 CaO

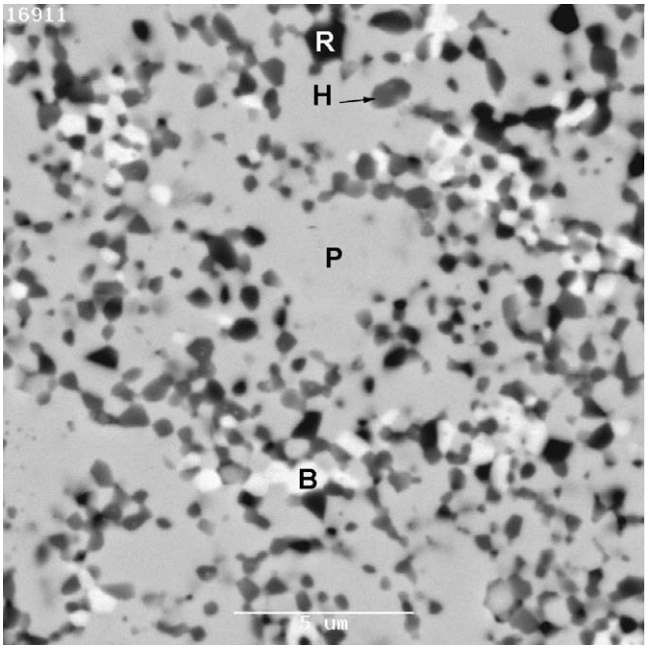

Fig. 1. Backscattered electron image of the baseline sample 2 (40 wt% UO_2). P = pyrochlore, H = hollandite, R = rutile and B = brannerite.

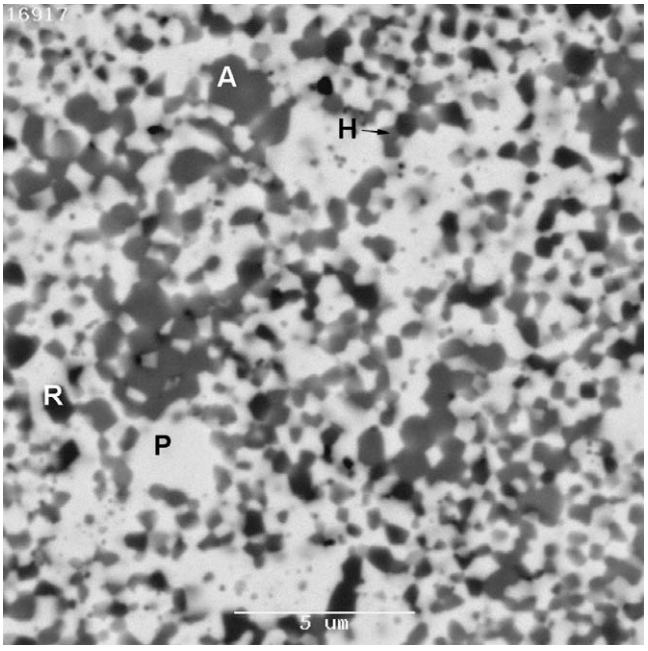

Fig. 2. Backscattered electron image of the sample 3 (30 wt% UO_2). P = pyrochlore, H = hollandite, R = rutile and A = perovskite.

perovskite is not unexpected in these two samples because using the same precursor material and adding less UO_2 than the baseline material, results in an excess of Ca (relative to that required to form pyrochlore). This excess Ca reacts with rutile to form perovskite ($CaTiO_3$). Fig. 2 shows the SEM backscattered electron image of the sample containing 30 wt% UO_2 which contained the same phase assemblage as the sample containing 35 wt% UO_2 but a different relative abundance of phases (see Table 2). The XRD phase analysis of the sample containing 45 wt% UO_2 (sample 4 in Table 1) showed it to consist of pyrochlore, rutile, hollandite and brannerite with their phase abundance shown in Table 2. Brannerite is the phase expected to form when all the available Ca has been used to form the pyrochlore phase [12]. The UO_2 left over in this process then reacts with the TiO_2 to form brannerite.

The EDS analyses of the pyrochlore phase in the 35, 40 and 45 wt% UO_2 samples were very similar with the composition of $CaU_{0.86}Zr_{0.14}Al_{0.05}Ti_{1.95}O_7$ being very close to the target composition (see above). The amount of Zr was slightly higher in the samples that contained <40 wt% UO_2 due to more Zr being available in the precursor material to enter the pyrochlore phase. The presence of the small amount of Al (as Al^{3+}) in the pyrochlore could be charge compensated for by the presence of a small amount of U^{5+} in addition to the targeted U^{4+} being present in the pyrochlore [18]. The EDS analysis of the pyrochlore phase in the sample containing 30 wt% UO_2 indicated that the Ca content was >1 formula unit (f.u.). The approximate composition was $Ca_{1.1}U_{0.7}Zr_{0.1}Al_{0.05}Ti_{1.95}O_7$ and other workers have reported pyrochlores with Ca contents of >1 f.u. [20–21]. This has been attributed to some of the U being in a valence state of >4+.

3.2. Varying the precursor material

The XRD phase analysis for the samples with increased TiO_2 (12 and 18 wt% excess to baseline composition, samples 5 and 6, respectively, in Table 1) showed them to consist of pyrochlore, rutile, hollandite and brannerite. In the 18 wt% excess rutile sample the pyrochlore content has been reduced to around 45 wt%, the rutile increased to ~26 wt%, hollandite ~12 wt% and the brannerite 17 wt%, compared with the baseline composition of 80 wt% pyrochlore, 10 wt% rutile and 10 wt% hollandite (see Table 2). The SEM backscattered image of this sample is shown in Fig. 3. The sample was fully dense with phases identified as above. The grain size was ~1 μm, similar to the other samples in this work. The effect of the excess TiO_2 in the above two samples means that there is less Ca and Zr available (see Table 1) to form the U-containing pyrochlore; this in turn means more TiO_2 is available to form brannerite and excess rutile.

The XRD phase analysis for the samples with increased TiO_2 and CaO (samples 7 and 8 in Table 1) showed them to consist of pyrochlore, rutile, perovskite and hollandite. The sample with 6 wt% excess in both TiO_2 and CaO (sample 7 in Table 1) contained ~75 wt% pyrochlore, ~9 wt% rutile, ~8 wt% hollandite and 8 wt% perovskite and the sample with 9 wt% excess in both TiO_2 and

Table 2
Estimated (mass fraction) phase assemblage of the samples.

Phase	Same precursor with different UO_2 content				Same UO_2 content with different precursor			
	Sample number 1 (%)	Sample number 2 (%)	Sample number 3 (%)	Sample number 4 (%)	Sample number 5 (%)	Sample number 6 (%)	Sample number 7 (%)	Sample number 8 (%)
Pyrochlore	77	71	69	76	49	45	75	64
Hollandite	14	10	13	13	12	12	8	11
Rutile	5	15	4	7	25	26	9	11
Perovskite	4	0	14	0	0	0	8	14
Brannerite	0	4	0	4	15	17	0	0

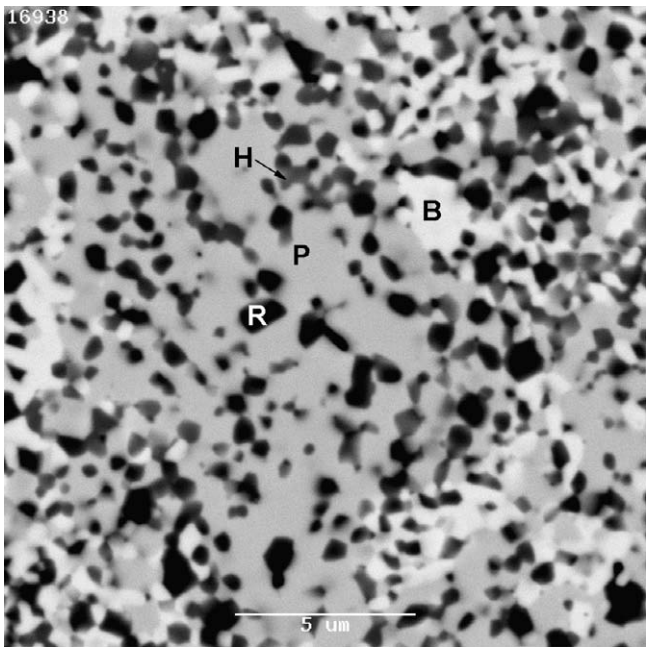

Fig. 3. Backscattered electron image of the sample 6 (18 wt% excess TiO_2). P = pyrochlore, H = hollandite, R = rutile and B = brannerite.

CaO (sample 8 in Table 1) consisted of 64 wt% pyrochlore, ~11 wt% rutile, ~11 wt% hollandite and 14 wt% perovskite (see Table 2). Fig. 4 shows the SEM image of the sample with 6 wt% excess TiO_2 and CaO (sample 7 in Table 1). The sample is dense with a grain size similar to the other samples (<1 μm), the phases identified were pyrochlore, perovskite, hollandite and rutile. The effect of adding excess TiO_2 and CaO was a reduction in the amount of pyrochlore phase relative to that in the baseline sample in favour of perovskite formation. The EDS analysis of the pyrochlore phase in the samples which contained excess TiO_2 indicated it to be close to the baseline composition. The EDS analysis of the pyrochlore phase in the samples with excess TiO_2 and CaO indicated that more than 1 f.u. of Ca was present ($Ca_{1.25}U_{0.7}Zr_{0.05}Al_{0.05}Ti_{1.95}O_7$). As mentioned above, for this pyrochlore composition to be correct, the average U oxidation state must greater than 4+.

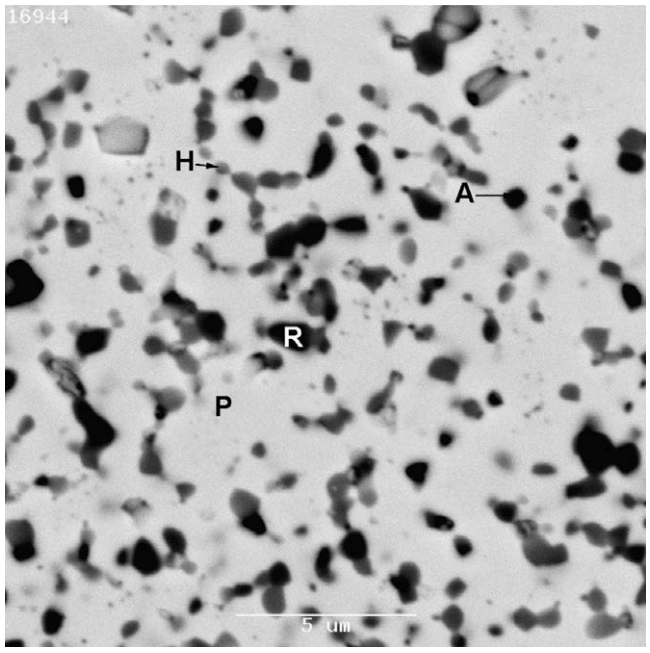

Fig. 4. Backscattered electron image of the sample 7 (6 wt% excess TiO_2 and CaO). P = pyrochlore, H = hollandite, A = perovskite and R = rutile.

3.3. Uranium oxidation state

DR spectra of uranium ions in polycrystalline pyrochlore have been reported previously [22] and it has been demonstrated that DR spectra can be used to identify U^{4+} and U^{5+} in pyrochlore. However, the DR spectrum of baseline sample 2 (not shown) did not show the expected spectrum for U^{4+} partly because the high abundance of U was such that the single-ion spectra were suppressed at the expense of pair interactions as in $(U_xTh_{1-x})O_2$ [23] as well as the dark nature of the sample. There is no indication of any U^{5+} present in the sample.

The DR spectrum of sample 7 is shown in Fig. 5. It is a typical spectrum of mixed valence states of uranium ions in pyrochlore with weaker absorption peaks from U^{4+} similar to the spectrum of U^{4+} in pyrochore [22], plus a sharp absorption peak at 6520 cm^{-1} attributable to U^{5+}. The presence of U^{5+} in this sample is consistent with the above EDS results. Although the U contents in samples 2 and 7 are the same, the relatively lower f.u. of U in the pyrochlore phase in sample 7 (0.7 f.u. compared to that of 0.86 f.u. in sample 2) has allowed the single-ion spectra of U to be measured.

The EELS measurement was carried out on two samples, the baseline sample, and sample 7 (see Table 1) which contained 6 wt% excess in both TiO_2 and CaO. The valence state of uranium in the baseline material was 4.13 ± 0.09. The error limits reported for these materials are ± one standard deviation of the data set (>6 measurements). Within the uncertainty in the EELS measurement, the measured value was consistent with the expected uranium valence state for this material (4.00), which in turn is consistent with the original design of the baseline waste form (see Section 1). The uranium valence state for sample 7, which contained excess TiO_2 and CaO, was 4.34 ± 0.06. This result supported the DRS measurements (Fig. 5) which showed the presence of U^{5+}. Although it is not possible to quantify DRS results, the valence state as measured by EELS appears to be qualitatively consistent with the DRS result. Assuming that uranium is present only in the 4+ and 5+ states (i.e., no 6+ is present), an average valence state of 4.34 corresponds to 66% U^{4+} and 34% U^{5+}. Note DRS cannot provide

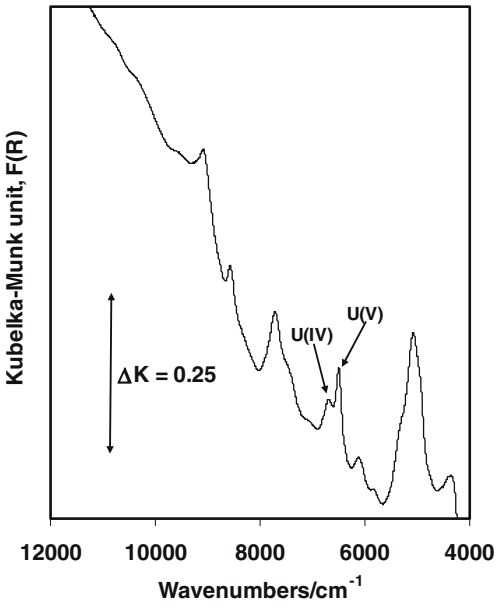

Fig. 5. Diffuse reflectance spectrum (4000–12,000 cm^{-1}) of sample 7.

Table 3
Normalised 7-day PCT releases for the elements in the samples.

Element	Same precursor with different UO_2 content				Same UO_2 content with different precursor			
	Sample number 1 (g/L)	Sample number 2 (g/L)	Sample number 3 (g/L)	Sample number 4 (g/L)	Sample number 5 (g/L)	Sample number 6 (g/L)	Sample number 7 (g/L)	Sample number 8 (g/L)
Al	0.11	0.15	0.13	0.20	0.11	0.19	0.09	0.16
Ba	0.06	0.11	0.14	0.05	0.35	0.09	0.04	0.07
Ca	0.03	0.03	0.02	0.04	0.04	0.03	0.02	0.02
Ti	5×10^{-6}	1×10^{-6}	3×10^{-6}	4×10^{-6}	4×10^{-6}	3×10^{-6}	4×10^{-6}	4×10^{-6}
U	2×10^{-5}	3×10^{-5}	2×10^{-5}	5×10^{-5}	2×10^{-5}	2×10^{-5}	3×10^{-5}	2×10^{-5}
Zr	8×10^{-5}	5×10^{-5}	3×10^{-5}	5×10^{-5}	6×10^{-5}	$7 \times 10^{--5}$	6×10^{-5}	7×10^{-5}

evidence for U^{6+} via sharp absorption peaks, because there are no *f* electrons in U^{6+}.

3.4. Leach testing

All samples were leach tested using the PCT procedure. Table 3 shows the normalised 7-day releases for the elements in the samples. There was no significant difference between the normalised releases for the elements in the samples and the normalised releases are comparable with those from synroc-C [13]. Yudintsev et al. [19] suggested that the presence of brannerite in waste forms will moderately lower the chemical durability of the waste form. In this case the small amounts of brannerite (4–17 wt%) would have had little effect on the durability of the waste form.

It is generally agreed that the leach resistance of synroc-C is very satisfactory. The phase constitutions of these samples contained the rutile and hollandite phases of synroc-C. The hollandite would immobilise Cs fission products. Sr fission products could react with rutile to form perovskite, in amounts too small to observe by XRD, for the samples which did not display perovskite. Rare-earth fission products and actinides other than U could readily enter both brannerite and pyrochlore, while the reducing conditions prevailing during HIPing would reduce Pd group elements and Tc to metal alloy particles as in synroc-C. Overall, the existing phase relationships contribute to the high chemical durability of the waste form materials.

Although the (7-day) PCT releases appear to be very low compared to those of the EA glass test reference material, PCT tests normally give lower leach rates, when 7-day releases are converted to g/m^2/day, than those derived from MCC-1 tests because of a relatively high sample surface area to leachate volume ratio in the PCT test which produces saturation effects. [It is readily calculated that the 7-day elemental leach rates in a PCT test for a sample of density of around 6 g/cm^3 – as in the present case – are around c/7 g/m^2/day, where c is the elemental release in g/L.]

4. Conclusions

Flexible pyrochlore-rich waste forms for uranium-rich radioactive waste streams have been developed. A baseline waste form using a 40 wt% UO_2 loading was developed. The influence of adjusting this baseline composition was then evaluated in two ways: (a) varying the UO_2 loading while keeping constant precursor oxide material, and (b) varying the precursor composition while keeping constant waste loading of UO_2. These changes had little effect on the durability of the waste form. There was no significant difference in the normalised release rates for the elements as a function of sample composition. The normalised release rates are comparable with those from synroc-C. The compositional variations resulted in the samples having a similar phase assemblage to the baseline composition, but the amounts of each phase varied. Compositional and phase analysis and EELS measurements showed that the oxidation state of the U in the baseline materials was close to 4+. Where more than 1 f.u. of Ca was present in the pyrochlore, DRS and EELS showed that this phase contained a mixture of U^{4+} and U^{5+}. These results show that the multiphase waste form developed here is highly effective in immobilising uranium containing wastes from radioisotope production, and is highly tolerant to variations in the precursor composition and waste/precursor ratios.

References

[1] Management of Radioactive Waste from ^{99}Mo Production, IAEA-TECDOC-1051, November 1998.
[2] G.L. Almeida, F. Helus, Radiochem. Radioanal. Lett. 28 (3) (1977) 205.
[3] Australian Atomic Energy Comm. Res. Establ., Technetium-99m Generators Prepared from Fission Produced Molybdenum-99, Quality Control and Performance Aspects, Lucas Heights, Australia, 1971.
[4] E.S. Gureev, S. Khuzhaev, A. Sultanov, N.A. Mirzaeva, U.T. Ashrapov, Uzbekskii Khimicheskii Zhurnal 6 (1990) 8.
[5] A. Mutalib, A.H. Gunawan, H. Lubis, R. Awaludin, Hamid, Sulaeman, K. Ishikawa, K. Sumiya, Y. Hishinuma, K. Yoshida, K. Tatenuma, in: JAERI-Conf, 2003-004, Proceedings of the 2001 Workshop on the Utilization of Research Reactors, 2003, pp. 202–210.
[6] O.P.D. Noronha, A.B. Sewatkar, R.D. Ganatra, C.K. Sivaramakrishnan, A.V. Jadhav, M.V. Ramaniah, H.J. Glenn, J. Nucl. Biol. Med. 20 (1) (1976) 32.
[7] V.S. Skuridin, E.V. Chibisov, Method and device for producing technetium-99m, Gos. Nauchnoe Uchrezhd. "Nauchno-Issled. Inst. Yadernoi Fiziki pri Tomskom Politekhnicheskom Univ. Min. Obrazovan. i Nauki RF", Russia, Application, RU, 2006, 7pp.
[8] V.S. Skuridin, A.I. Ryabchikov, V.M. Golovkov, E.A. Nesterov, E.V. Chibisov, Method of manufacture of the chromatographic generator of technetium-99m from irradiated by neutrons molybdenum-98, Gos. Nauchnoe Uchrezhd. "Nauchno-Issledovatel'skii Institut Yadernoi Fiziki pri Tomskom Politekhnicheskom Universitete Ministerstva Obrazovan. i Nauki, Russia, RU, 2006, 6pp.
[9] Z. Yen, Y. Han, P. Zhang, Y. Li, S. Wang, Yuanzineng Kexue Jishu 20 (2) (1986) 129.
[10] A.E. Ringwood, S.E. Kesson, N.G. Ware, W. Hibberson, A. Major, Nature 278 (5701) (1979) 219.
[11] S.E. Kesson, A.E. Ringwood, Radioact. Waste Manage. Nucl. Fuel Cycle 4 (2) (1983) 159.
[12] E.R. Vance, M.L. Carter, S. Moricca, T.L. Eddowes, Ceram. Trans. 168 (Environmental Issues and Waste Management Technologies in the Ceramic and Nuclear Industries X) (2005) 225.
[13] A.E. Ringwood, S.E. Kesson, K.D. Reeve, D.M. Levins, E.J. Ramm, Synroc, North-Holland, New York, 1988.
[14] PCT is Based on the ASTM Designation: C 1285-02 Standard Test Methods for Determining Chemical Durability of Nuclear, Hazardous, and Mixed Waste Glasses and Multiphase Glass Ceramics: The Product Consistency Test (PCT).
[15] W.W. Wendlandt, H.G. Hecht, Reflectance Spectroscopy, Wiley Interscience, New York, 1966.
[16] M. Colella, G.R. Lumpkin, Z. Zhang, E.C. Buck, K.L. Smith, Phys. Chem. Miner. 32 (2005) 52.
[17] M.W.A. Stewart, E.R. Vance, A. Jostsons, K. Finnie, R.A. Day, B.B. Ebbinghaus, Mater. Res. Soc. Symp. Proc. 713 (2002) 381.
[18] E.R. Vance, G.R. Lumpkin, M.L. Carter, D.J. Cassidy, C.J. Ball, R.A. Day, B.D. Begg, J. Am. Ceram. Soc. 85 (7) (2002) 1853.
[19] S.V. Yudintsev, T.S. Yudintseva, in: Proceedings of the International Conference on Radioactive Waste Management and Environmental Remediation, 8th, Bruges, Belgium, Sept 30–Oct 4, 2001, 1 (2002) 547–551.
[20] M.W.A. Stewart, E.R. Vance, A. Jostsons, B.B. Ebbinghaus, J. Austral. Ceram. Soc. 39 (2) (2003) 130.
[21] Y. Zhang, K.P. Hart, M.G. Blackford, B.S. Thomas, Z. Aly, G.R. Lumpkin, M.W. Stewart, P.J. McGlinn, A. Brownscombe, Mater. Res. Soc. Symp. Proc. 663 (2002) 325.
[22] Y. Zhang, E.R. Vance, K.S. Finnie, B.D. Begg, M.L. Carter, Royal Soc. Chem. (2006) 343.
[23] E.R. Vance, Y. Zhang, J. Nucl. Mater. 357 (1–3) (2006) 77.